Power quality enhancement of wind farm based on DFIG entirely interfaced with distribution network during symmetrical and unsymmetrical voltage faults

[1]OUNISSA Aouchenni, [1]RABAH Babouri, [1]DJAMAL Aouzellag, [2]FERHAT Chabour, [2]CRISTIAN Nichita

[1]University of BEJAIA-ALGERIA; Laboratoire de Maitrise des Energies Renouvelables, E-Mail: aouchenni.ounissa@gmail.com.
[2]University of Le Havre, Le Havre-France; Groupe de Recherche en Electrotechnique et Automatique, GREAH Lab.

Abstract: *The purpose of this paper is to describe a novel approach for voltage control of radial electrical distribution network with connected wind farm in presence of symmetrical and unsymmetrical faults. The proposed method is based on the wind farm induction generators entirely interfaced with the distribution network. The proposed structure performs better than the conventional one due to the ability of the suggested structure to increase the generator power until twice its nominal power. Consequently, the system size and cost are reduced; the disturbances do not affect the doubly fed induction generators (DFIGs) and coupling of these generators to the network is improved. A reliable control strategy for the grid side converter is developed in order to restrain the disturbances caused by grid voltage fault and to ensure the stability of the system, regarding power quality and voltage level. Obtained results show the effectiveness of the proposed method in mitigating the disturbances caused by voltage faults and in minimizing system transmission losses while providing best voltage levels.*

Key words: *DFIG, voltage faults, voltage regulation, radial distribution network, wind generation, power control.*

1. Introduction

Due to the fluctuating nature of the wind, the power quality and stability of an electrical network can be affected when high wind power integration is present. Therefore, high penetration rate of wind energy into a power systems, which were build based on large synchronous generators, may lead to a convenient redesign of the power system [1, 2]. The main objective of this work is the voltage control of radial electrical networks integrating wind farm based on DFIGs. The stator and the rotor of each generator are connected to the common DC link bus through two rectifiers as shown in figure 1; the grid inverter side is sized to the total wind farm power. Electrical distribution networks were not designed to deal with significant power injections from wind energy conversion system (WECS); therefore the anticipated proliferation of WECS results in a number of network planning and operational challenges, including voltage control, protection issues, altered transient stability, bidirectional power flow and increased fault levels; voltage variation has been identified as one of the dominant effects [3].

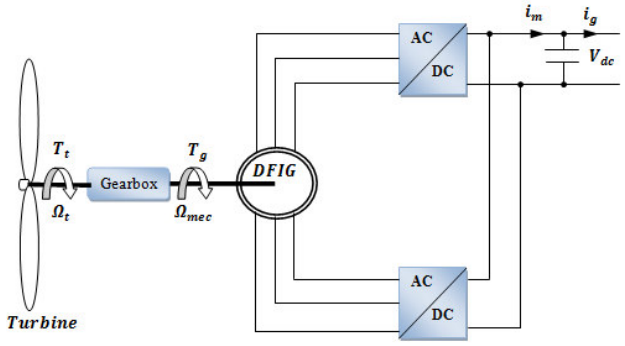

Fig.1 – DFIG entirely interfaced with network.

As a result, a lot of papers such as [4] and [5] discussed the problem of WECS connection in electrical networks. The integration impacts of a wind power on the voltage stability and the powers forwarded into the lines of electrical network are presented in [6]. Voltage quality disturbances such as voltage dips pose a serious concern as a power quality problem, since due to their stochastic nature they cannot readily be eliminated from regular utility systems. However, they can be mitigated. In this paper, a novel approach to voltage control for radial electrical distribution networks with connected wind farm during voltage dip is proposed.

2. Wind generator model

A modeling methodology of torque and power characteristics for a wind turbine is used according to [8, 9]. The algorithm allows to:

- Generate the power coefficient characteristics as a function of the speed ratio λ and the pitch angle of blades β:

$$C_P = C_P(\lambda, \beta) \quad (1)$$

-Generate the available wind power Pt as a function of the wind speed V_w, the rotation speed Ω_t and the pitch angle of blades β:

$$P_t = P_t(V_w, \Omega_t, \beta) \quad (2)$$

-calculate the available turbine torque $T_t$as a function of the wind speed V_w, the rotation speed Ω_t and the pitch angle of blades β:

$$T_t = T_t(V_w, \Omega_t, \beta) \quad (3)$$

In this work pitch angle β is fixed to 0 (β =0). Figure 2 shows power coefficient and figure 3 shows the wind power for variable wind speed.

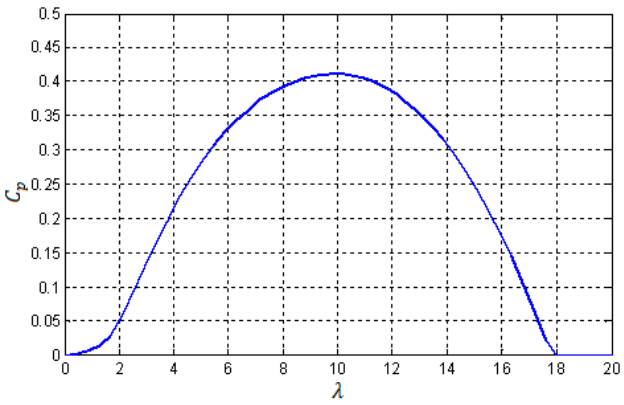

Fig.2 – Power coefficient.

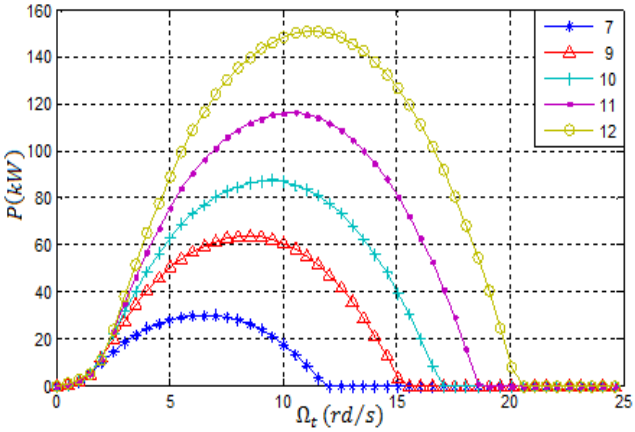

Fig.3 – Wind power for variable wind speed.

3. DFIG model and vector control

The classical electrical equations of the DFIG in the PARK frame are written as follows:

$$\begin{cases} v_{sd} = R_s i_{sd} + s\varphi_{sd} - \omega_s \varphi_{sq} \\ v_{sq} = R_s i_{sq} + s\varphi_{sq} + \omega_s \varphi_{sd} \\ v_{rd} = R_r i_{rd} + s\varphi_{rd} - (\omega_s - \omega)\varphi_{rq} \\ v_{rq} = R_r i_{rq} + s\varphi_{rq} + (\omega_s - \omega)\varphi_{rd} \end{cases} \quad (4)$$

Where R_s and R_r are, respectively, the stator and rotor phase resistances.

$\omega = p.\Omega_{mec}$ is the electrical speed, p is the number of pair pole and s is Laplace operator. In our case we choose the direction of reference (d, q) according to the direct stator flux vector φ_{sd} , so the model of steady DFIG will be simplified as follows:

$$\begin{cases} v_{sd} = R_{sd} i_{sd} \\ v_{sq} = R_s i_{sq} + \omega_s \varphi_{sd} \\ v_{rd} = R_r i_{rd} - \omega_r \varphi_{rq} \\ v_{rq} = R_r i_{rq} + \omega_r \varphi_{rd} \end{cases} \quad (5)$$

Such as:

$$\omega_r = \omega_s - \omega \quad (6)$$

These simplifications lead to the reference currents expression:

$$i_{sq-ref} = \frac{T_{em-ref}}{p\varphi_{ref}},\ i_{rq-ref} = \frac{-L_s}{M} i_{sq} \quad (7)$$

The machine magnetization is assured equally by the stator and the rotor side, so:

$$i_{sd-ref} = i_{rd-ref} = \frac{\varphi_{sref}}{M + L_s} \quad (8)$$

The control bloc diagram of the DFIG is shown in figure 4. The models of network link, converters and DC bus have been developed in [11].

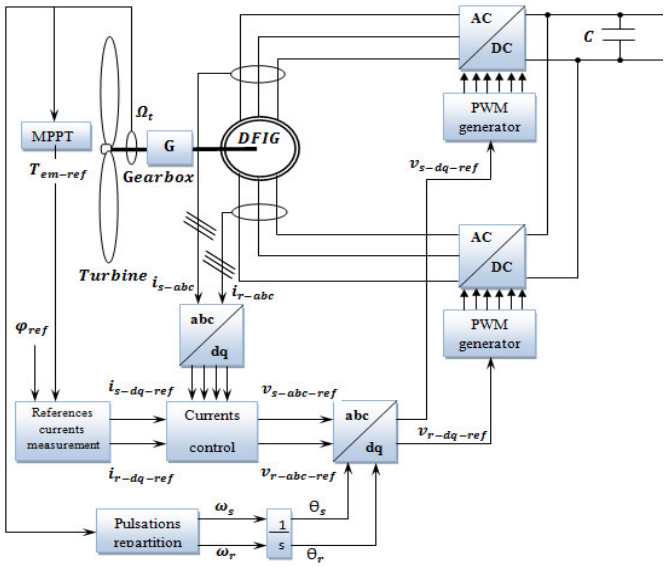

Fig.4 – Control diagram of aero generator.

4. Grid side converter control strategy

The essential part for well-performance of controller in inverter is the voltage detection circuit. Voltage must be detected fast and regulated. The voltage disturbance detection method is based on the error between the reference voltage magnitude V_{ref} imposed equal to 10kV and voltage magnitude measured V_{mea} on the network. The controller system is presented in figure 5. The three phase supply voltage is transformed from abc to odq frame using Park transformation. Phase Locked Loop (PLL) is used to track supply voltage phase. The output of the PLL ($\Theta = \int \omega dt$) is used to compute the direct-axis and quadrature-axis components of the AC three phase voltage and currents [10].

Where:

$$V_S = \sqrt{{V_{Sd}}^2 + {V_{Sq}}^2} \quad (9)$$

When voltage dip or voltage drop is detected, the inverter switches into active mode to react as fast as possible to inject a quantity of reactive power Q_{ref} in order to provide the best voltage profile in the system as well as to minimize the system transmission losses. Therefore the injection reactive power is generated according to the difference between the reference voltage and the measured voltage and it is applied to the converter to produce the preferred voltage profile, using the voltage control based on fuzzy controller [7].

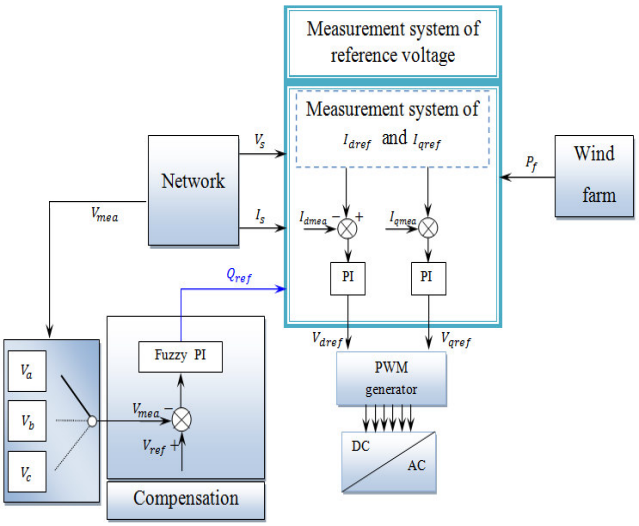

Fig.5 – Control block-diagram of the grid-side converter.

The reference active power P_{ref} is imposed equal to the power generated by wind farm. The active and reactive powers forwarded are given by equations 10 and 11 respectively.

$$P = V_{Sd} I_{Sd} + V_{Sq} I_{Sq} \quad (10)$$

$$Q = V_{Sq} I_{Sd} - V_{Sd} I_{Sq} \quad (11)$$

Park components of the reference currents are given by equations 12 and 13.

$$I_{dref} = \frac{P_{ref} V_{Sd} + Q_{ref} V_{Sq}}{{V_{Sd}}^2 + {V_{Sq}}^2} \quad (12)$$

$$I_{qref} = \frac{P_{ref} V_{Sq} - Q_{ref} V_{Sd}}{{V_{Sd}}^2 + {V_{Sq}}^2} \quad (13)$$

Where:

I_{dref}, I_{qref} : Park components of the reference currents;

V_{dref}, V_{qref} : Park components of the reference voltages;

P_{ref}, Q_{ref} : Active and reactive powers references;

V_{Sd}, V_{Sq} : Park components of V_S;

V_{mea} : Voltage measured.

5. Studied system

The wind farm consists of seven 75 kW induction generators entirely interfaced with a 10 kV distribution network. The network consists of a centralized source of power P_S equal to 3 MW, This source is connected to a load with inductive behavior through an electrical line of impedance $Z = R + j\,X$, electrical study network is illustrated in figure 6 and the system data is given in appendix. A wind farm is considered to be connected to load bus and will be generate to the network a power P_f at an integration rate between 30% and 40%.

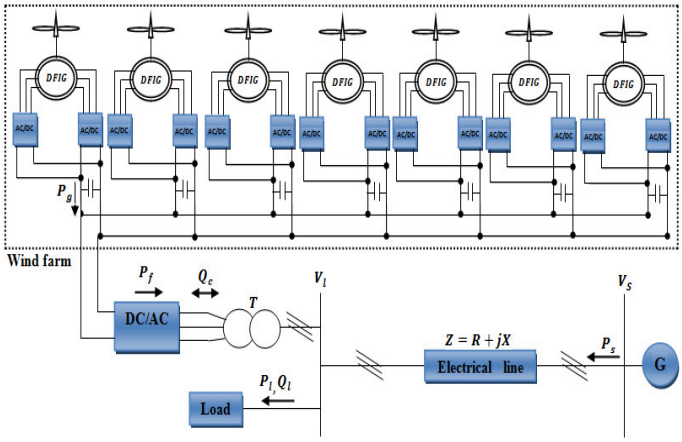

Fig.6 – Diagram of the studied system.

6. Simulation results and discussion

6.1 Electrical distribution network before and after integration of wind farm

First, we will study the electrical distribution network without compensation to evaluate power losses and voltage drop before and after integration of the wind farm. Figure 7 shows the evolution of the active power losses in the line before $P_{losse-bef}$ and after $P_{losse-aft}$ integration of wind farm and figure 8 shows the voltage drop before $V_{drop-bef}$ and after $V_{drop-aft}$ integration of the wind farm.

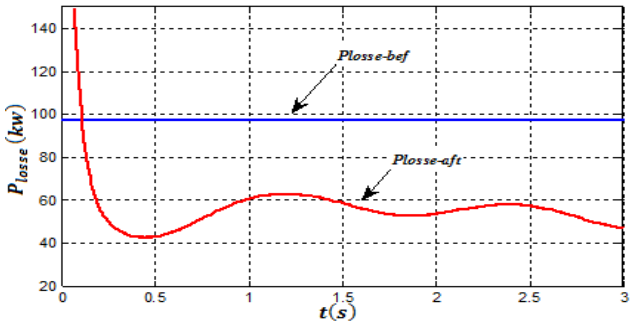

Fig.7 – Active power losses in the line after and before integration of wind farm.

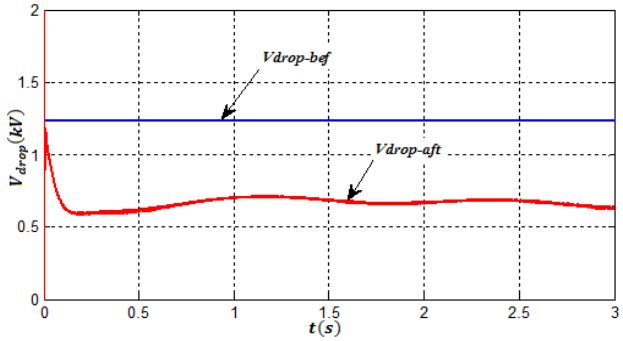

Fig.8 – Voltage drops in the line after and before integration of wind farm.

The simulation results show high power losses and high voltage drop in the line. This is caused mainly by the inductive load. Reactive power required by inductive load increases the line current and the increase in line current causes the overload of the source also voltage drop and power losses. Wind farm connected to network is one of the solutions used to solve the voltage drop problem and power losses through producing power at this location of the deficit. So the wind farm is connected in bus load. A significant improvement of the active power losses is noted in figure. We can also see through figure 8 that the voltage drops are decreased. Figure 9 illustrates the speed of the DFIG Ω_{mec}, as we can notice that the machine operates in a wide range of speed variation, up to twice its nominal speed.

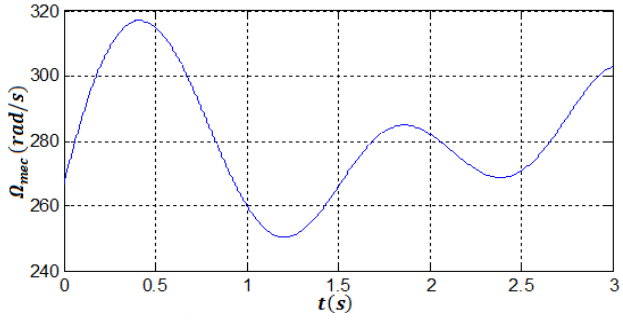

Fig.9 –DFIG rotor speed.

The electromagnetic torque of the DFIG T_{em} and the reference torque T_{em-ref} are given by figure 10; in fact the electromagnetic torque varies with the rotational speed variation of the machine.

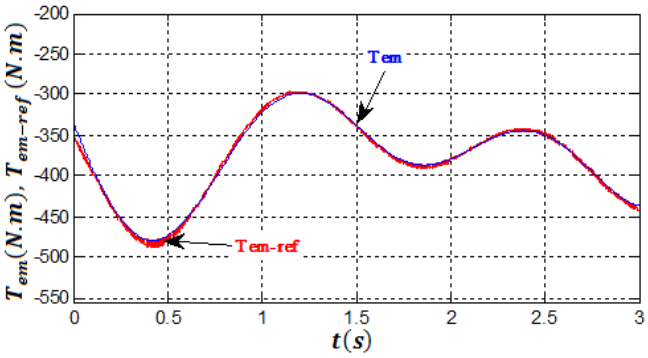

Fig.10 – Electromagnetic torque and its reference value.

The stator P_s, rotor P_r, turbine P_t and generator P_g powers of WECS are shown in figure 11 as we can see that the power injected into the grid equal to the mechanical power provided by the wind turbine, of course without taking into account the different losses.

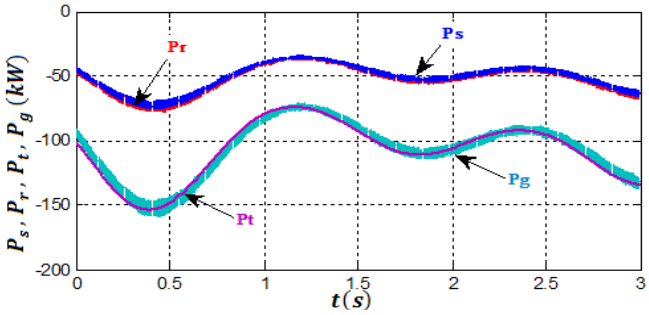

Fig.11 – Stator, Rotor, Turbine and generator powers.

Figure 12 shows the regulation of the DC link voltage.

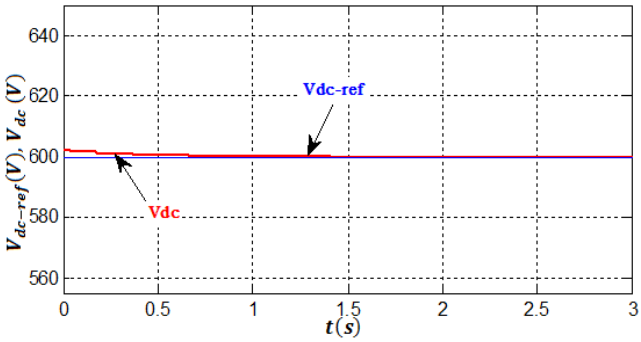

Fig.12 – DC link voltage and its reference value.

Figure 13 shows the active power P_l and reactive power Q_l at the load node and figure 14 presents the

active powers provided by source and wind farm.

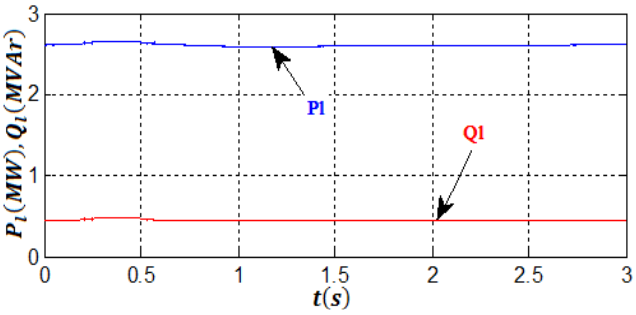

Fig.13 – Active power and reactive power at the load bus.

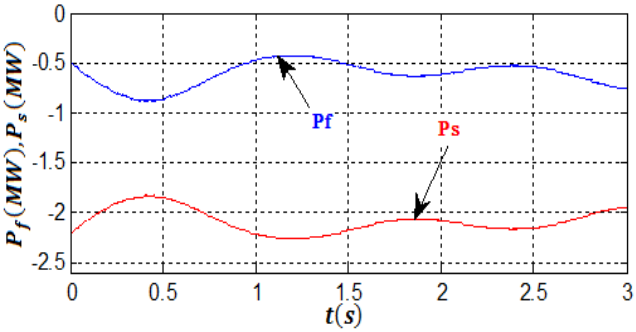

Fig.14 – Active power of the source and wind farm.

6.2 Electrical distribution network with voltage fault

In order to solve the problem of voltage and power fluctuation caused by the power delivered by wind farm, and especially to restrain the disturbance caused by grid voltage fault and to provide a best voltage profile in the system, control of grid-side inverter will be made to provide reactive power necessary to regulate voltage and powers flows. The results obtained show the contribution of the compensation to mitigate voltage fault and regulate the voltage profile on the network as well as powers at load node.

6.2.1 Symmetrical voltage fault-voltage dip

A voltage dip V_{dip} occurs on the network with a sudden rectangular voltage change of 1400ms duration and voltage reduction of 20%. Voltage depression is shown in figure 15.

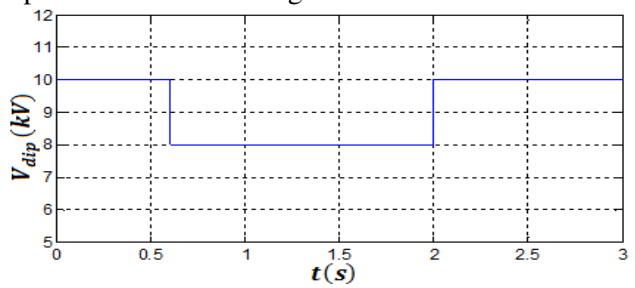

Fig.15 – Voltage dip.

Figure 16 presents the evolution of the voltage magnitudes at the load node before V_{l-bef} and after V_{l-aft} compensation, the voltage became stable.

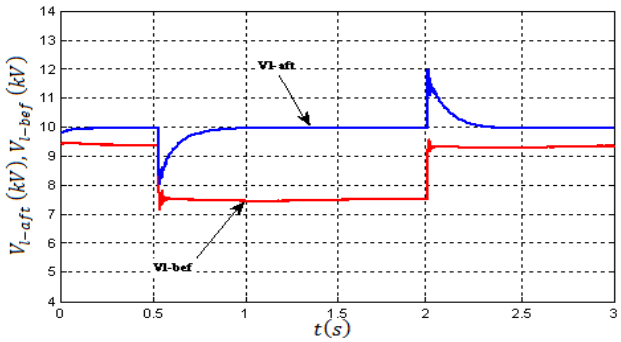

Fig.16 – Voltage magnitudes at load node before and after compensation.

Figure 17 illustrates the evolution of the active and reactive powers at the load node after compensation.

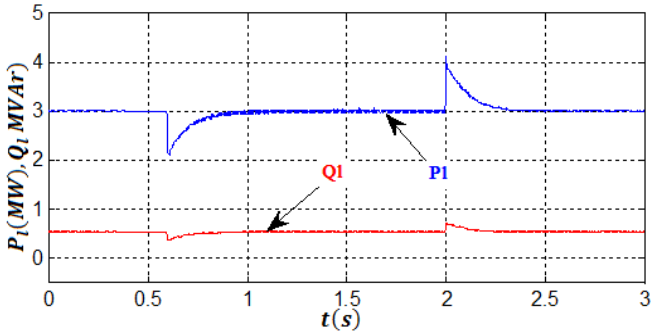

Fig.17 – Active power and reactive power at the load node after compensation.

Figure 18 illustrates the active P_c and reactive powers Q_c at connecting node of wind farm, clearly shows the interest of the compensation, where the reactive power varies according to the change of active power and voltage, for maintain better voltage profile in the electrical distribution network.

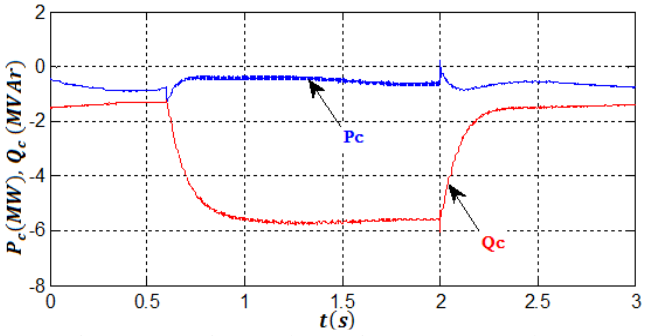

Fig.18 – Active and reactive powers at the connecting node of the farm.

6.2.2 Symmetrical voltage fault-voltage drop

A higher voltage drop V_{drop} occurs on network with a reduction of 30% as observed on figure 19.

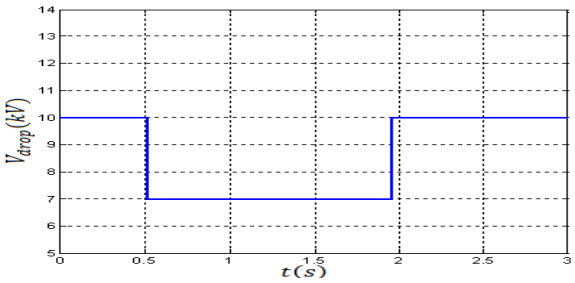

Fig.19 – Voltage drop.

Figure 20 shows the evolution of the voltage magnitudes at the load node V_{l-aft} after compensation. As in the previous scenario, there is a significant voltage drop. However, due to the injection of reactive power by compensation, the final voltage in load node is stabilized. In this way, the network is supported during the voltage drop.

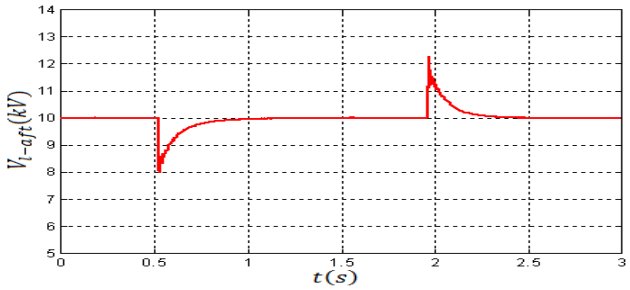

Fig.20 – Voltage magnitudes at load node after compensation.

Figure 21 shows the evolution of the active P_{l-bef} and reactive Q_{l-bef} powers at the load node before compensation as well as active P_{l-aft} and reactive Q_{l-aft} powers after compensation.

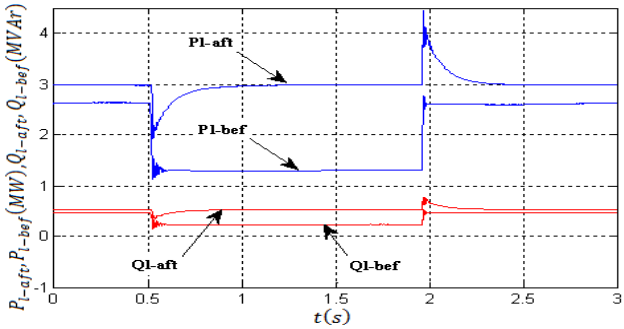

Fig.21 – Active powers and reactive powers at the load node before and after compensation.

The active and reactive powers at load node are compensated.

6.2.3 Unsymmetrical voltage fault

Figure 22 present the three phase voltages waveforms with 30% voltage drop in phase "a".

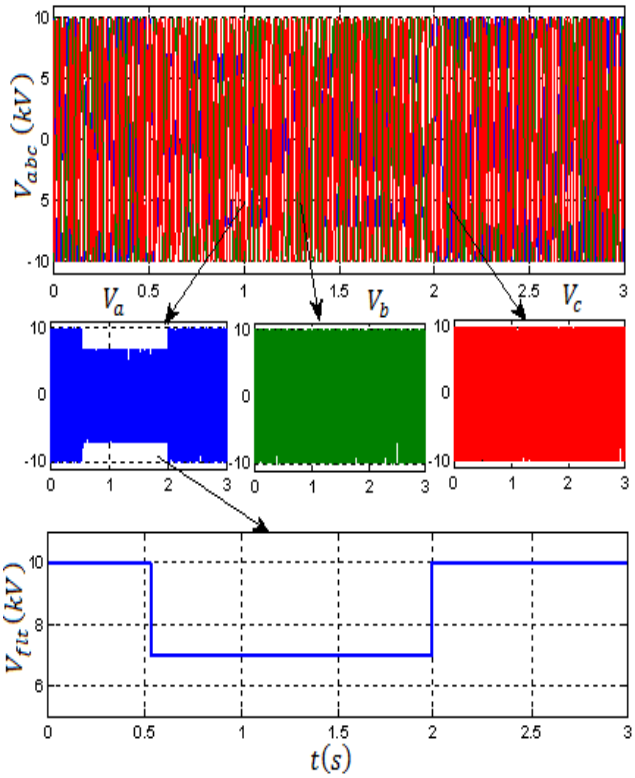

Fig.22 – Three phase voltages waveforms and voltage depression.

Figure 23 presents the evolution of the voltage magnitudes at the load node before V_{l-bef} and after V_{l-aft} compensation, the voltage is stabilized.

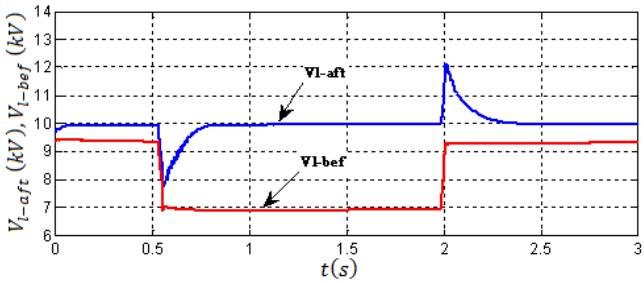

Fig.23 – Voltage magnitudes at load node before and after compensation.

The control strategy to voltage profile regulation in the distribution network has been verified with a symmetrical voltage dip, symmetrical voltage drop and unsymmetrical voltage drop.

7. Conclusion

In this paper the capability of grid-side inverter control of compensating different voltage faults has

been studied and tested on a radial distribution network to which a wind farm is connected. Voltage faults compensation performances in an electrical network as well as the problems induced by wind power on the voltage profile are exposed. Simulations were done and the results were presented. Some advantages of the proposed control include voltage dip, voltage drop and unsymmetrical faults mitigated, load voltage stabilized, system transmission losses minimized. The simulation results are shown also that the proposed voltage dip compensator can provides continuous power to load.

Appendix

WECS parameters
G=30; R=10.5m; f =0.0024N.m.s/rd; j=100kg.m2;
Ls=0.0154H; *Lr*=0.0154H; M=0.0151H; p=2;
Pn= 75kW; *Rs*=0.03552Ω; *Rr*= 0.02092Ω;
Un=400V.
Load parameters
P=3MW, Q=1.58MVAr.
Line parameters
r= 0.5Ω/km; x=1.57Ω/km; l= 5km; R=r. l;
X=x. l; l=length of the line.

Acknowledgments

This paper was finalized during my scientific internship performed in GREAH laboratory. The results will be experimentally validated using the real time simulator based on HILS concept developed at GREAH [13, 14].

REFERENCES

1. Ackerman T. Wind Power in Power Systems. Royal Institute of Technology Stockholm, Sweden: John Wiley & Sons, 2005.
2. Mathur RM, Varma RK. Thyristor-based FACTS controllers and electrical: transmission systems. John Wiley & Sons, 2002.
3. Boynuegri A.R, Vural B, Tascikaraoglu A, Uzunoglu M, Yumurtacı R. Voltage regulation capability of a prototype Static VAr Compensator for wind applications. Applied Energy 2012, 93:422–431. Science Direct, Elsevier.
4. Aouzellag Lahaçani N, Aouzellag D, Mendil B. Static compensator for maintaining voltage stability of wind farm integration to a distribution network. Renewable Energy 2010, 35:2476–2482. Science Direct, Elsevier.
5. Aouzellag N, Aouzellag D, Mendil B. Contribution to the improvement of voltage profile in electrical network with wind generator using SVC device. Renewable Energy 2010, 35: 243–248. Science Direct, Elsevier.
6. Roy N.K, Pota H.R, Hossain M.J. Reactive power management of distribution networks with wind generation for improving voltage stability. Renewable Energy 2013, 58: 85-94. Science Direct, Elsevier.
7. Aouchenni O, Aouzellag D, Aouzellag N. Voltage regulation of wind farm connected to distribution network using fuzzy supervisory control. International Journal of Scientific & Engineering Research, Volume 4, Issue 12, December-2013.
8. Nichita C**.** Etude et développement de structures et lois de commande numériques pour la simulation en temps réel d'actionneurs. Application à la réalisation d'un simulateur d'aérogénérateur de 3 kW. PhD Thesis, University of Le Havre, 1995.
9. Diop. A.D, Nichita C., Belhache J.J, Dakyo B, Ceanga E. Modeling Variable Pitch HAWT Characteristics for Real Time Wind Turbine Simulator. Wind Engineering Journal, vol 23, No. 4, p. 225-243, 1999.
10. Ghedamsi K, Aouzellag D. Improvement of the performances for wind energy conversion systems. Electrical Power and Energy Systems 2010, 32:936-945. Science Direct, Elsevier.
11. Babouri R, Aouzellag D, Ghedamsi K. Integration of doubly fed induction generator entirely interfaced with network in a wind energy conversion system. Energy Procedia 2013, 36: 169 – 178. Science Direct, Elsevier.
12. Zhang X-P, Handschin E, Yao M. Multi-control functional static synchronous compensator (STATCOM) in power system steady-state operations. Electric Power Systems Research 2004, 72: 269–78.
13. Caraiman G, Nichita C, Mînzu V, Dakyo B, Jo C. H. Concept study of offshore wind and tidal hybrid conversion based on real time simulation. Renewable Energy and Power Quality Journal 2011, RE&PQJ-8 ISSN 2172-038X.
14. Stevenson P, Cristian N, M.B CAMARA, Brayima D. Control strategy of a wind turbine simulation system designed for an hybrid wind-tidal real time emulator, 3rd Renewable Power Generation Conference (RPG™), 24 - 25 September 2014, Naples, Italy.